



## Open Archive Toulouse Archive Ouverte

OATAO is an open access repository that collects the work of Toulouse researchers and makes it freely available over the web where possible

This is an author's version published in: <http://oatao.univ-toulouse.fr/28687>

### **To cite this version:**

Martin, Elodie Catherine and Khazaka, Rabih and Martineau, Donatien and Azzopardi, Stephane and Alexis, Joël  *Direct heat sink printing on metallized ceramic substrate for power electronics applications: heat treatment identification and its impacts.* (2020)  
In: 11th International Conference on Integrated Power Electronics Systems, 24 March 2020 - 26 March 2020 (Berlin, Germany).

Any correspondence concerning this service should be sent to the repository administrator: [tech-oatao@listes-diff.inp-toulouse.fr](mailto:tech-oatao@listes-diff.inp-toulouse.fr)

# Direct heat sink printing on metallized ceramic substrate for power electronics applications: heat treatment identification and its impacts

Elodie MARTIN<sup>1</sup>, Rabih KHAZAKA<sup>2</sup>, Donatien MARTINEAU<sup>2</sup>, Stephane AZZOPARDI<sup>2</sup>, Joël ALEXIS<sup>1</sup>

<sup>1</sup>LGP, INP-ENIT 47 avenue d'Azereix BP 1629 65016 Tarbes Cedex, France

<sup>2</sup>SAFRAN SA, Safran Tech Department of Electrical and Electronic Systems 78114 Magny les Hameaux, France

## Abstract

The aim of this paper is to evaluate a new packaging technology developed for high power density and harsh environment power module applications. The assembly was achieved using Selective Laser Melting (SLM) technique in order to directly print  $AlSi_7Mg_{0.6}$  alloy heat sinks on the back side of direct bonded aluminum metallized substrate. Thermal simulations were conducted in order to evaluate the potential benefit of this technology. Results show a reduction of more than 22% of the junction to ambient thermal resistance compared to conventional structure. Experiments were conducted on both aluminum and nickel finish metallization of the Direct Bonded Aluminum (DBA) substrates. The assemblies were studied under several scales from the metallurgical and mechanical study of the interfaces to the measurement of the macroscopic strains of the substrates. The heat treatment temperature of 250°C has been identified based on the hardness versus temperature curve of the  $AlSi_7Mg_{0.6}$  alloy. After a stress relieve thermal treatment of 2 hours at 250°C, the warpage of highly deformed substrates with printed heat sink is reduced significantly (more than 30% in some cases) without altering the metallurgy and the mechanical properties of the interfaces for both Ni and Al finish layers. The thermal conductivity of the printed alloy is improved by about 20% at temperatures below 100°C after the heat treatment.

## 1 Introduction

In order to achieve mass and volume gain in power converters, an increasing interest to use high density integrated power electronics modules in harsh environment has emerged. This trend is mainly pushed by the market introduction of high temperature wide band-gap Silicon Carbide (SiC) or Gallium Nitride (GaN) power semiconductor devices with junction temperature theoretically exceeding 200°C. However, robust assemblies with high performance cooling systems are needed to insure the operation capability of the electronic systems.

Metal Additive Manufacturing (AM) has proved to be a growing area of research in the near past years to achieve optimized heat sink designs [1][2]. Conventional power module can then be thermally coupled to the high performance additive manufactured heat sinks to improve the thermal management. The thermal coupling is conventionally achieved using organic Thermal Interface Material (TIM) like thermal grease, elastomer films or phase changing films. However, TIMs suffer from their high thermal resistance and limited stability at high temperatures [3]. In order to take the full advantages of additive manufacturing technologies and bypass the aforementioned limitations related to TIM, a new approach consists in directly printing heat sinks using SLM technique on the back side metalization of the ceramic metallized substrate [4]. However, since the metal powder is melted for short periods during the process, high residual stresses are induced in the assembly during manufacturing. In order to reduce the amount of residual stress, while maintaining good dimensional and physical stability, Stress Relieving Heat Treatment (SRHT) is commonly performed on the SLM parts after the AM process. The SRHT reduces the ultimate tensile strength of the as-built parts to a great extent while increases the ductility level.

Various studies have evaluated the impact of commonly used thermal treatments (T6 or T4) on the mechanical and microstructure properties of the bulk Al alloys based part [5][6]. However, those treatments are achieved at high temperatures (>400°C) that are not compatible for our assembly since they can induce the fracture of the brittle ceramic.

The aim of this paper is to propose a soft stress relieve thermal treatment and evaluate its impact on the thermal properties of the printed material and on the mechanical and microstructural properties of the interfaces between the printed material and the substrate. The substrate warpage was also evaluated for various heat sink designs before and after heat treatment in order to establish a relationship between the printed pattern and the induced residual stress for the pristine and heat treated assemblies. Before discussing the experimental tests and associated results, and in order to evaluate the potential improvement in term of junction-to-ambient thermal resistance of the proposed approach, thermal simulations performed on the directly printed heat sinks on metallised substrates and on a conventional one are presented hereafter.

## 2 Thermal simulations

A 1200V -50A phase leg inverter power module, composed by two switching cells electrically connected in series, has been used in this part. Each switching cell is composed from a SiC MOSFET transistor and a SiC Schottky diode. The power losses within the MOSFET and the diode were considered to be 40W and 20W respectively. The detailed material properties and thicknesses of the assembly and the cooling fluid (air) used in the simulations are listed in Table 1. The reference heat sink is used in the simulation to compare the thermally coupled substrate to independent heatsink using TIM with the proposed structure where the heat sink is directly printed on the substrate. The base of the reference heat sink

is considered to be 0.8 mm thick. The thermal coupling between the reference heat sink and the DBA substrate is ensured by a 100 $\mu$ m thick thermal grease with a thermal conductivity of 2W/mK.

Table 1: Material properties used in the thermal simulation

	Thickness (mm)	$\lambda$ (W/mK)	Cp (J/kg.K)	$\rho$ (kg/m <sup>3</sup> )
SiC	0.2	300	510	4360
Solder	0.1	30	600	9000
Al	0.4	202	871	2719
AlN	1	150	400	3300
AlSiMg	29	125	890	2630
TIM	0.1	2	1000	2000
Air	30	0.025	1006	1

In order to have a fair comparison between the two simulated structures, the heat sink mass and occupied volume were kept constant. The top view of the simulated power module as well as the cross section of the two simulated structures are illustrated in Figure 1.

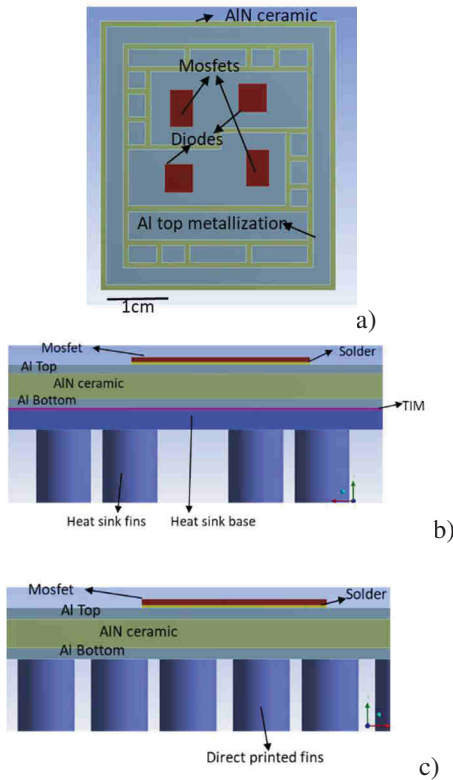


Figure 1: Schematics showing (a) the top view of the simulated power module, (b) the cross section of conventional assembly and (c) the cross section of the assembly with directly printed heat sink on the substrate bottom metallization. The two assemblies have the same weight but the pin fins number is higher in (c) than (b) since unlike (b), (c) does not include a base for the heat sink.

The inlet air coolant temperature was 20°C. The density and heat capacity were 1kg/m<sup>3</sup> and 1006J/kgK respectively. To reduce the model complexity, some assumptions have been considered: the natural convection, the radiation as well as the roughness of the surface of the heat sink have been neglected. In addition, the variation of the air properties as function of temperature has not been taken into account. The 3D steady governing equations for

conjugate heat transfer based on Navier-Stokes equations combined with continuity equation, energy equation and momentum equations were solved using ANSYS® Fluent implicit Solver. The turbulent  $k$ - $\epsilon$  standard model with enhanced wall treatment was used. The convergence criteria for the residual  $x$ ,  $y$  and  $z$  direction velocity and the residual of energy equation were set to 10<sup>-3</sup> and 10<sup>-6</sup> respectively.

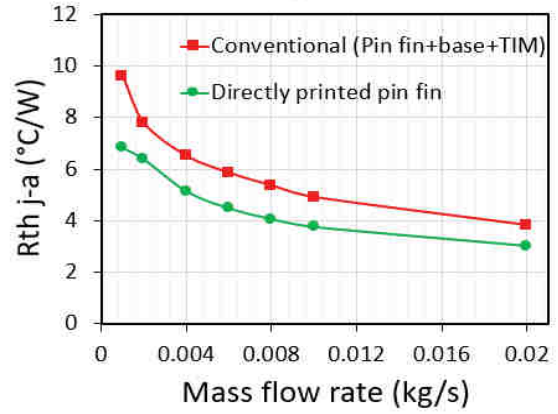


Figure 2: Junction-to-ambient thermal resistance as function of air mass flow rate for conventional (red) and proposed assembly (green).

The junction-to-ambient thermal resistance ( $R_{th_{j-a}}$ ) of the power module assembly versus the air mass flow rate for the conventional package (TIM and reference heat sink) and the proposed direct printed pin fins on the substrate is illustrated in Figure 2. For the two above mentioned cases, the thermal resistance is reduced by 27% at a mass flow rate of 0.001kg/s and 22% for the flow rate of 0.02kg/s. The cooling performance improvement when direct heat sink printing is used can be explained by the complete elimination of the low thermal conductivity TIM and the increase of the heat transfer area at iso-mass heat sinks (due to the suppression of the heat sink base).

### 3 Experiments

In this work, commercially available Direct Bonded Aluminum (DBA) metallized substrates were used. The dimensions of the AlN ceramic and Al metal layers were 48×42×1mm<sup>3</sup> and 46×40×0.4mm<sup>3</sup> respectively. Al layers were bonded on both sides of the ceramic plates and the pattern is then realised by selective etching of the top substrate metal layer. The substrates were chosen for their high thermomechanical reliability, good thermal conductivity, and the compatibility of the Al metallization with the printed AlSi<sub>7</sub>Mg<sub>0.6</sub> alloy [7][8]. For some samples, and in order to investigate the impact of the finish layer on the interfaces properties, a 5 $\mu$ m thick Ni metallization layer was plated on the substrates metallization (Ni-P with P content between 8 to 12%). The laser melting apparatus SLM 280HL was used to print the AlSi<sub>7</sub>Mg<sub>0.6</sub> metal parts. The particle size of the AlSi<sub>7</sub>Mg<sub>0.6</sub> powder is in the range of 20 $\mu$ m up to 60 $\mu$ m. The 3D geometry is realized layer by layer using a 350W laser power with a scan speed of 600mm/s and 900mm/s for the edge contour and the center of the built parts respectively. The laser beam locally melts the powder which is quickly solidified to form the slice.

Powder layers are deposited and melted consequently until the achievement of the final design. An argon atmosphere is maintained in the chamber during the whole process in order to limit the oxidation of metallic materials and to prevent fire. The supporting plateau is heated at a temperature of 150°C in order to reduce the residual stresses in the assembly. Figure 3 presents various printed pattern on 15 substrates fixed on the sole after the powder removal.

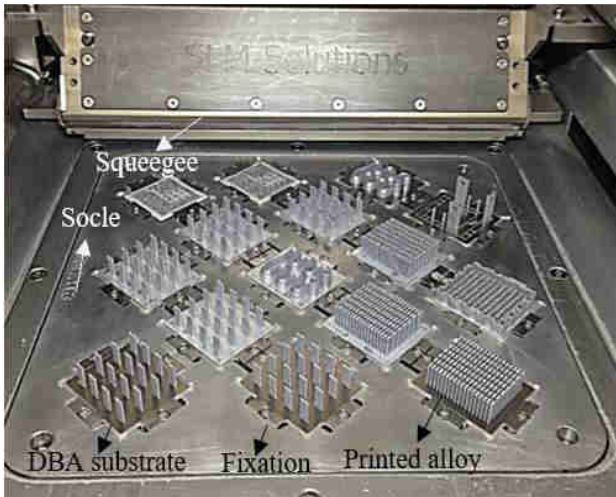


Figure 3: Directly printed patterns on the DBA substrates fixed on the supporting plateau after the powder removal at the end of the process.

The DBA substrates printed with rectangular fins were used for microstructural and mechanical interfaces evaluation while the ones printed with heat sink were used for the substrates warpage evaluation (Figure 4). Substrates without any printed part are used as reference.

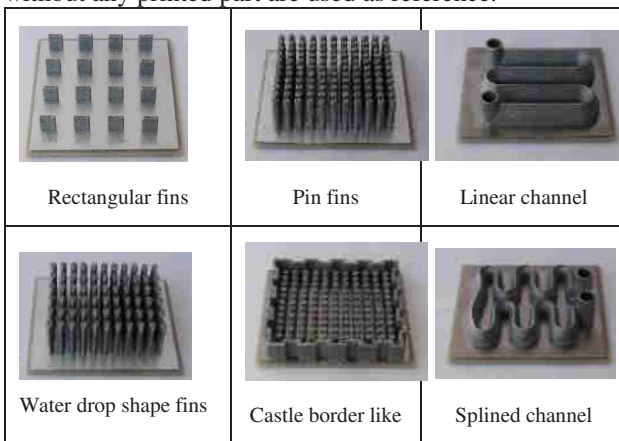


Figure 4: Various printed patterns on substrates used in this study.

The microstructure and interface properties have been characterized using a ZEISS EVO HD15 SEM (Scanning Electron Microscopy) after preparation and Keller etching. The interfaces mechanical properties have been characterized in shear test using the INSTRON 33R4204 apparatus. The head of the equipment was in contact with the surface of the substrate and the mechanical tests were carried out with a force cell of 10kN and a displacement speed of 1mm/min. For each condition, three tests were performed to verify the measurements repeatability. Hardness measurements have been performed from room temperature until 350 °C using a ZWICK 250 dcaN . The used load is fixed at 0.5. The approach speed varies

between 0.2 and 0.25mm/min. The 10 seconds charging time is followed by a 10 second stage and finally unloading.

The density has been evaluated at room temperature using the mass and the volume measurements. For the thermal diffusivity and the specific capacity, the flash method in the temperature range between 20°C and 200°C has been used. Finally, the warpage of the substrates has been measured on the width and on the length of the substrates by using a WYKO NT1100 optical profilometer in white light. For each dimension, three independent measurements (with two measurements on the borders and one on the substrate center) have been performed and the mean value was calculated and presented.

## 4 Results and discussion

### a) Heat treatment definition

In order to define the SRHT, the hardness evolution as a function of the temperature is defined for the printed alloy (Figure 5). Based on the obtained results, a heat treatment of 2h at 250°C was selected since it does not drastically change the metallurgy and causes a small decrease in hardness of about 20 %, which reduces the residual stresses while keeping acceptable mechanical strength.

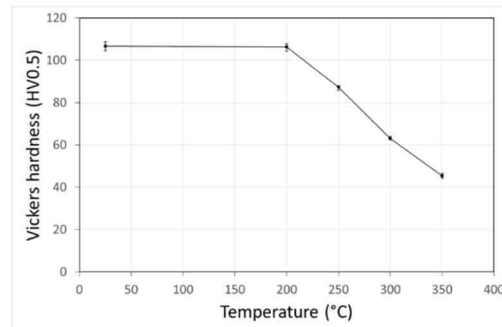


Figure 5: Material hardness as function of temperature. Bars represent the standard deviation.

### b) Impact of the heat treatment on thermal conductivity of the printed alloy

The printed alloy density of 2630kg.m<sup>-3</sup> was measured at room temperature while its specific capacity and its thermal diffusivity were measured in the temperature range between 20°C and 200°C. The thermal conductivity  $k$  was then calculated by multiplying the diffusivity, the density and the specific capacity.

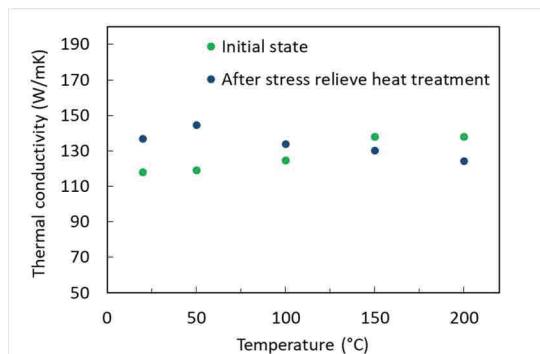


Figure 6: Thermal conductivity versus temperature at the initial state and after the stress relieve heat treatment.

$k$  values of  $125\text{W}\cdot\text{m}^{-1}\cdot\text{K}^{-1} \pm 10\%$  were deduced in the temperature range between  $20^\circ\text{C}$  and  $200^\circ\text{C}$  at the initial state and after the SRHT. This value is on the same range of as built cast alloy  $120\text{-}140\text{ W}\cdot\text{m}^{-1}\cdot\text{K}^{-1}$ . At temperatures below  $100^\circ\text{C}$ , the thermal conductivity of the printed alloy is improved by about  $20\%$  after the SRHT (Figure 6).

### c) Impact of the heat treatment on interfaces properties

At the initial time  $t_0$ , the interfaces with Al and Al-Ni finish are very similar from a metallurgical point of view and both of them show a low void and defect ratio with the substrate metallization. After the heat treatment, the interfaces do not show significant modification apart the detection of some rich Ni-P precipitate regions at the interface between the diffusion zone and the wall when Ni finish is used (Figure 7)

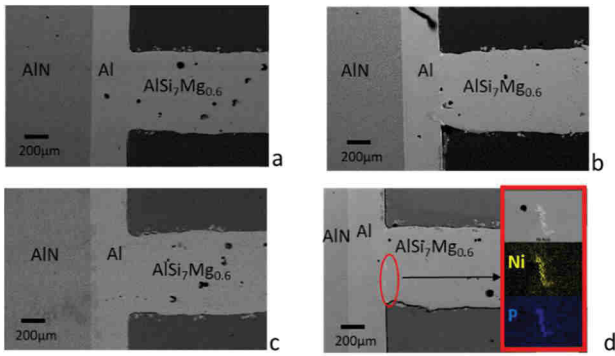


Figure 7: SEM images for the interfaces (a) Al at  $t_0$  (b) Al-Ni finish at  $t_0$ , (c) Al after thermal treatment and (d) Al-Ni finish after thermal treatment with focus region and EDX detection of precipitates.

The mechanical properties of the interfaces were evaluated using the shear test before and after the SRHT for both Al and Al-Ni finish layers. As presented in Figure 8, the influence of SRHT and the nature of the finish layer do not

seem to have any effect on the mechanical strength of the interfaces and shear stress values of about  $100\text{ MPa}$  were measured. Those stress values are considered to be largely sufficient for our applications since the main role of the printed parts is the related to the thermal management and the latter will not be submitted to hard mechanical solicitations.

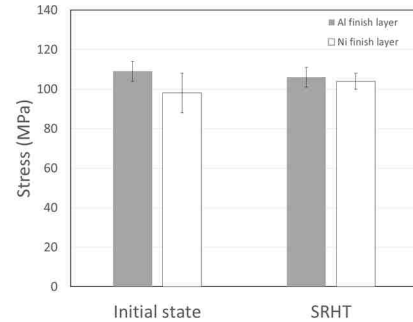


Figure 8: Shear stress values for Al and Al-Ni finish layer before and after stress relieving heat treatment (SRHT).

The fractured surfaces were analyzed before and after SRHT by SEM, EDX and also by using profilometry in order to identify the type and the location of fracture (Figure 9). SEM and EDX analysis show a ductile fracture with a large amount of Al without Si at the surface that suggests two potential failure types: a cohesive fracture in the Al or an adhesive fracture at the interface between the Al and the printed alloy diffusion zone. The relief indicates a depth of about  $250\mu\text{m}$ . Combined the SEM profile showing a maximum diffusion depth of alloy elements in the first  $200\mu\text{m}$  of the Al substrate metallization, it can be deduced that the fracture rather corresponds to a cohesive rupture in the Al substrate metallization. The same results were obtained for Al and Al-Ni finish layer before and after the SRHT.

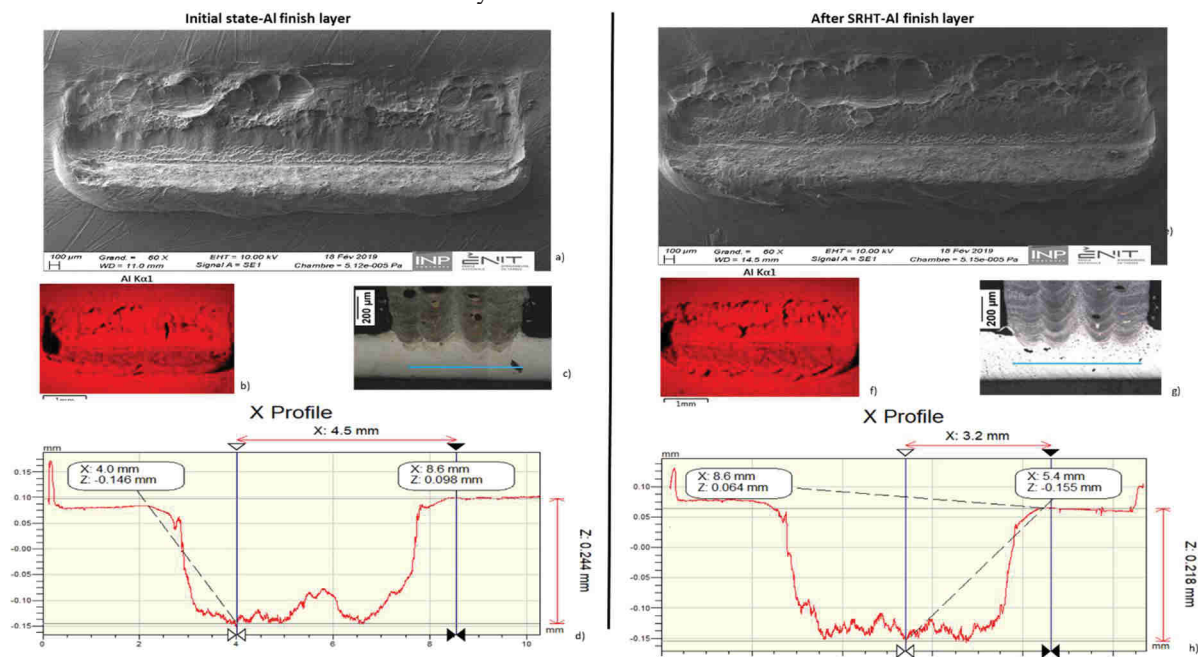


Figure 9: Measurement at initial state: (a) SEM image of the substrate fractured surface, (b) Al element mapping at the fractured surface, (c) fracture position indicated by blue line on cross section view before shear tests and (d) depth measurement of the fractured location. Measurement after SRHT: (e) SEM image of the substrate fractured surface, (f) Al element mapping at the fractured surface, (g) fracture position indicated by blue line on cross section view before shear tests and (h) Depth measurement of the fractured location.

#### d) Impact of optimized heat treatment on substrate warpage

The effect of the heat treatment (2h at 250°C) on the stress relaxation was evaluated by measuring the substrate deformation obtained before and after SRHT for naked substrates and substrates with direct printed heat sink (Figure 10). Results show that naked substrates or matrix fins heat sinks geometries (water drop shape fins and pin fins) have deformations of about 50µm. For geometries with long linear printed vectors: castle border like, linear channel, and splined channel, the deformation can exceed 150µm and can even go beyond 250µm in the worst case. The warpage is much more pronounced in the same axis of the linear printed vector and heterogeneities of deformations are observed for the geometries with linear and splined channels. In fact, decreasing the length of scanning vectors reduces the residual stresses and hence the warpage of the substrate. This can be due to two favorable mechanisms: the local division and redistribution of the stresses in the X and Y directions once the melted metal solidifies; the better distribution of the heat that serves as local preheating and leads to a reduction in the thermal gradient.

After the heat treatment, substrates which were initially slightly deformed, do not show significant modification. On the other hand, the heat treatment reduces the camber in both directions for the substrates that were significantly deformed. This stress relaxation is related to the creep of the aluminum based alloy at about 40% of its melting temperature.

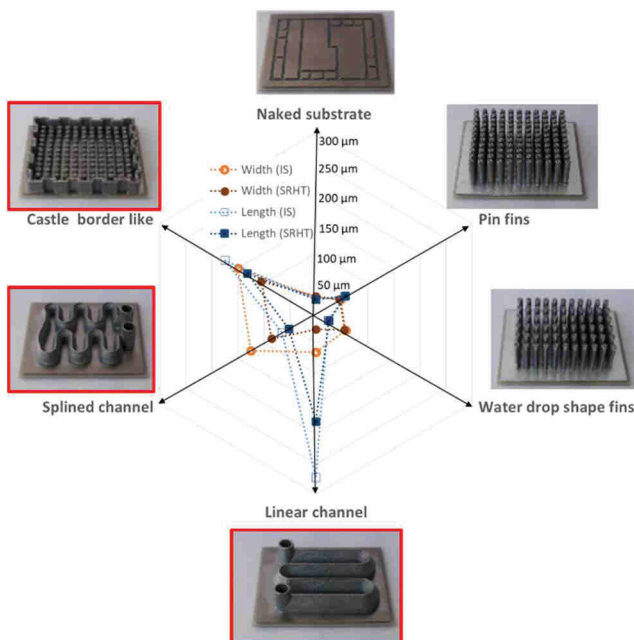


Figure 10: Comparison between initial state (IS) and after stress relieving heat treatment (SRHT) warpage measurements. Red borders surround the substrates that present deformation higher than 100µm in at least one direction.

## 5 Conclusion

Directly printing heat sinks using SLM technique on the back side of the ceramic metallized substrate offers an improvement of more than 22% in term of junction to ambient thermal resistance and allow to bypass the issues related to thermal interface material. However high residual stresses can be induced in the assembly due to the manufacturing process. This study allowed the definition of a stress relieving heat treatment of 2h at 250°C to reduce the warpage in the power electronics assembly where the heat sinks are directly printed on the substrate. The selected heat treatment allows the improvement of the thermal conductivity of the printed alloy by about 20% at room temperature. The interfaces between the laser melted AlSi<sub>7</sub>Mg<sub>0.6</sub> alloy and the substrate Al metallization do not show any voids or fracture after the fabrication process and the heat treatment. High mechanical adhesion with shear strength values exceeding 100MPa have been measured at the initial state and after the stress relieve thermal treatment on both Al and Al-Ni finish layer. Under shear tests, ductile fractures take place in the bulk of Al substrate metal layer in all the cases. Finally, during the SRHT the creep effect takes place and allows the warpage reduction of more than 30% in the case of significantly cambered substrates.

## References

- [1] E.M. Dede, S.N. Joshi, and F. Zhou. Topology Optimization, Additive Layer Manufacturing, and Experimental Testing of an Air-Cooled Heat Sink. *Journal of Mechanical Design*, 137, 2015.
- [2] M. Wong, I. Owen, C.J. Sutcliffe, and A. Puri. Convective heat transfer and pressure losses across novel heat sinks fabricated by Selective Laser Melting. *International Journal of Heat and Mass Transfer*, 52:281–288, 2009.
- [3] R. Skuriat, J.F. Li, P.A. Agyakwa, N. Matthey, P. Evans, and C.M. Johnson. Degradation of thermal interface materials for high-temperature power electronics applications. *Microelectronics Reliability*, 53:1933–1942, 2013.
- [4] R. Khazaka, D. Martineau, T. Youssef, T. L. Le and S. Azzopardi, Direct Printing of Heat Sinks, Cases and Power Connectors on Insulated Substrate Using Selective Laser Melting Techniques, 69th Electronic Components and Technology Conference (ECTC), Las Vegas, USA, May 2019.
- [5] E. Brandl, U. Heckenberger, V. Holzinger, D. Buchbinder, Additive manufactured AlSi10Mg samples using Selective Laser Melting (SLM): microstructure, high cycle fatigue, and fracture behavior, *Material Design* 34: 159-169, 2012.
- [6] F. Trevisan, F. Calignano, M. Lorusso, J. Pakkanen, A. Aversa, E.P. Ambrosio, M. Lombardi, P. Fino and D. Manfredi, On the Selective Laser Melting (SLM) of the AlSi10Mg Alloy: Process, Microstructure, and Mechanical Properties, *Materials*, 10, 76, 2017.
- [7] R. Khazaka, L. Mendizabal, D. Henry, R. Hanna, Survey of high-temperature reliability of power electronics packaging components, *IEEE Transactions on Power Electronics*, Vol. 30, No. 5, May 2015.
- [8] A. Lindemann, G. Strauch, Properties of direct aluminum bonded substrates for power semiconductor components, *IEEE Transactions on Power Electronics*, Vol. 22, No. 2, 2007.